

International Journal of Scientific Research and Reviews

Oral Squamous Cell Carcinoma Classification using Deep Boltzmann Machine and GLCM Features

J. Indhumathi^{1*} and P. Dhanalakshmi²

¹Dept. of CSE., Annamalai University, Annamalainagar - 608002, Tamil Nadu, India.

²Dept. of CSE., Annamalai University, Annamalainagar - 608002, Tamil Nadu, India.

ABSTRACT

In this paper, a new methodology for automatic oral cancer detection system is proposed. The incidence of oral cancer is highest worldwide and also the prevalence is lower in women than men. Squamous Cell Carcinoma is one amongst the foremost tumor of oral cavity. Oral Squamous Cell Carcinoma disease identification through pc vision approach may be a new introduced technique in era. Each variant features a distinctive histomorphological appearance. Thus, the method is designed to identify the histopathological variants of OSCC and it's according to the morphological appearance with Deep Boltzmann machine. This method is having three major steps: Preprocessing, Feature Extraction and Classification. The Preprocessing step involves image acquisition of microscopic images and image enhancement is done using median filter. In this paper, automatic detection of few types of cancer diseases are to be considered using DWT and GLCM. Discrete Wavelet Transform (DWT) is used for multi band decomposition, once the image gets segmented then, the Gray-Level Co-occurrence Matrix (GLCM) method is applied to extract the features in terms of statistical texture-based. The deep learning based Neural Network, RBM classifier is used to classify the result, and then result is compared with the existing system of Oral classification using ANN result shows better accuracy.

KEYWORDS: Oral Squamous Cell Carcinoma(OSCC), Adenoid Squamous Cell Carcinoma(ASCC), Basaloid Squamous Cell Carcinoma(BSCC), Papillary Squamous Cell Carcinoma(PSCC), Sarcomatoid Carcinoma(SC), Verrucous Carcinoma(VC), Discrete Wavelet Transform(DWT), Gray Level Co-Occurrence Matrix, Deep Belief Network(GLCM), Restricted Boltzmann Machines(RBM), Artificial Neural Network(ANN).

Corresponding Authors

***J. Indhumathi,**

PG Scholar,

Department of Computer Science and Engineering,

Annamalai University,

Annamalainagar- 608002, Tamil Nadu, India.

Email : hasinindhu5@gmail.com, Ph: 9488876549.

INTRODUCTION

Squamous cell carcinoma is far and away the foremost vital and also the additional normally malignant membrane tumor of the top and neck hard the over 90% malignancies. Conventional Oral Squamous Cell Carcinoma (OSCC) can present as multi variants that make up in quantum about 10-15% of all squamous cell carcinomas (SCC). Conventional oral squamous cell carcinoma (OSCC) will give as multi variants that conjure in quantum about 10-15 of all epithelial cell carcinoma¹. These variants include) Adenoid Squamous Cell Carcinoma (ASCC), Basaloid SCC (BSCC), papillary SCC (PSCC), Verrucous Carcinoma (VC) and Sarcomatoid Carcinoma (SC). Each of these variants has a unique histomorphological appearance⁴.

Adenoid Squamous cell carcinoma (ASCC)

Adenoid squamous cell carcinoma is a rare variant of squamous cell carcinoma with features of adenoid pattern. It has been reported to originate in the sun- exposed skin of the head and neck region. Although rare, there are cases documented within the oral cavity and nasopharynx. The clinical behavior and the prognosis are variable. We report a case of adenoid squamous cell carcinoma in a 63-year-old female patient with a large mass in the left mandibular alveolar ridge².

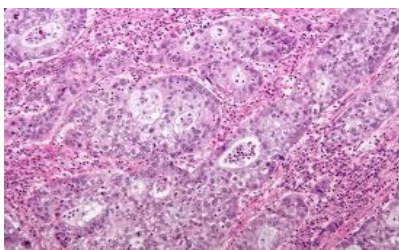


Figure 1: Adenoid squamous Cell Carcinoma

Basaloid Squamous Cell Carcinoma (BSCC)

More than 90 percent of cancers that occur in the oral cavity and oropharynx are squamous cell carcinoma. Normally, the throat and mouth are lined with so-called squamous cells, which are flat and arranged in a scale-like way. Squamous cell carcinoma means that some squamous cells are abnormal⁶.

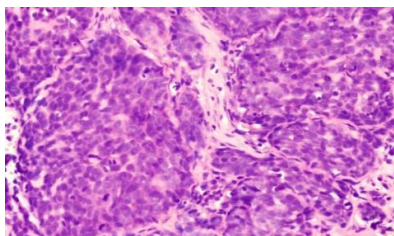


Figure 2: Basaloid Squamous Cell Carcinoma

Papillary Squamous Cell Carcinoma(PSCC)

Oral papillary squamous cell carcinoma (PSCC) is an unusual variant of squamous cell carcinoma with a better prognosis. The most common location of PSCC in the oral cavity is the gingiva and buccal mucosa, and it is exceedingly rare in the tongue. Herein, we present a case of PSCC in an 85-year-old male with a history of heart transplant and long-term use of immunosuppression medication. A verrucouspedunculated mass measuring 3.5 cm in the greatest dimension was present on the tip of tongue and a partial glossectomy was performed.

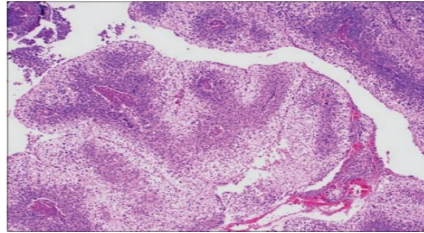


Figure 3: Papillary Squamous Cell Carcinoma

Verrucous Carcinoma(VC)

About 5 percent of all oral cavity tumors are verrucous carcinoma, which is a type of very slow-growing cancer made up of squamous cells. This type of oral cancer rarely spreads to other parts of the body, but can invade the tissue surrounding the site of origin⁵.

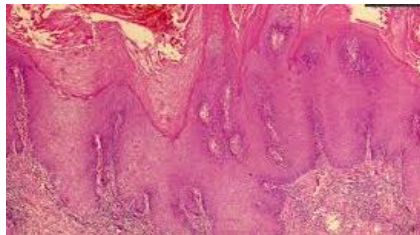


Figure 4: Verrucous Carcinoma

Sarcomatoid Carcinoma (SC)

Sarcomatoid carcinoma (SC) is an uncommon variation of squamous cell carcinoma which is portrayed by a dysplastic epithelial segment and a stromal component with obtrusive fusiform or axle formed cells. The clinical and histopathologic qualities make it exceptionally hard to recognize SC from epithelioid sarcoma (ES). We present an instance of a 51-year-elderly person with a delicate tissue mass in the oral hole analyzed as proximal variation of epithelial sarcoma on incisional biopsy.

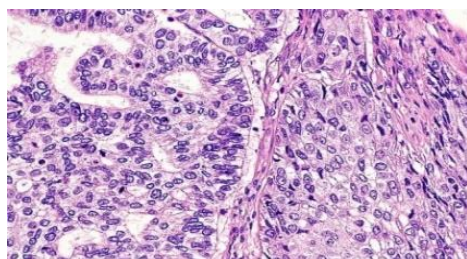


Figure 5: Adenoid Squamous Cell Carcinoma

But Adeno Squamous Cell Carcinoma is a aggressive disease with 60 % of patients die of this disease. Figure 6 : Shows the overall architecture of the proposed classification System.

PROPOSED METHODOLOGY

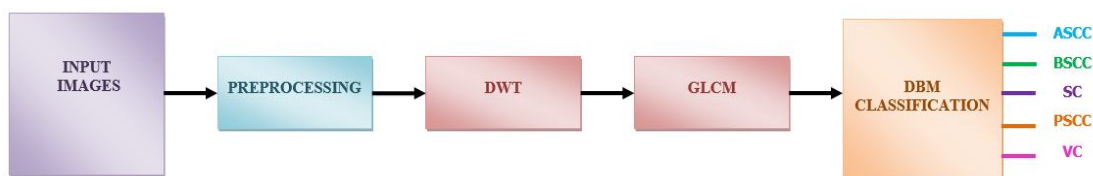


Figure 6: Block Diagram of Histological Variants of OSCC Classification System

PRE-PROCESSING

Minuscule pictures are multidimensional as far as imaging edge. Pictures are brought from top-down, left-right, and front back perspectives. The informational index utilized in this module had its best quality and most total pictures from the front-back point of view. The informational index utilized in this module had its best quality and most total pictures from the front-back point of view. For preprocessing stage, we utilized a procedure of three phases depicted, yet with little adjustments.

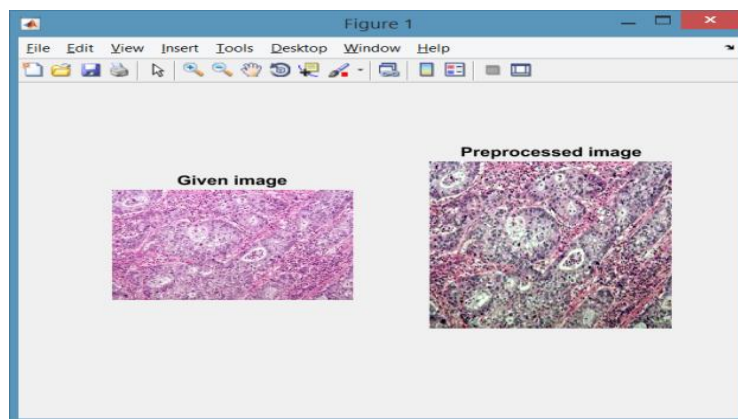


Figure 7: Preprocessed image of the given image

Rather than deferring normal image age, we performed it first. This technique had the accompanying favorable circumstances on the preprocessing: the nature of the last picture higher is

saved, in light of the fact that unique images with best quality were utilized to create the normal image, instead of adjusted pictures. The time required for informational collection preprocessing is decreased, since each occurrence was spoken to by one picture rather than set of images. This diminished informational collection size to 1/8 of its unique size. In this technique, Noise is smothered utilizing middle sifting. Image is improved utilizing max channel.

FEATURE EXTRACTION

Discrete Wavelet Transform (DWT) is any wavelet transform for which the wavelets are discretely sampled. The key advantage is it captures both frequency and location information. The discrete wavelet transform (DWT) is a linear transformation that operates on a data vector whose length is an integer power of two, transforming it into a numerically different vector of the same length. DWT is computed with a cascade of filtering followed by a factor 2 sub-sampling.

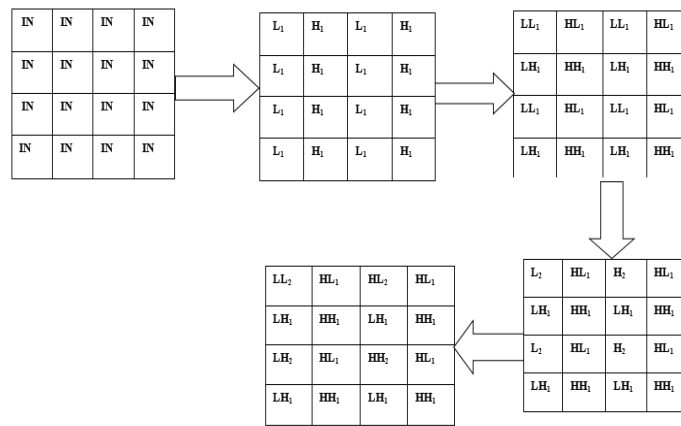


Figure 8: Decomposition of DWT

$$HH_{j+1}[n][col] = \sum_{i=0}^{N_H-1} h[i] \times H_j[2n - 1 - i][col]$$

Where $j=\{0,1,\dots,L-1\}$, $row = \{0,1,\dots,N/2^j - 1\}$, $m=\{0,1,\dots,M/2^{j+1} - 1\}$, $col = \{0,1,\dots,N/2^{j+1}-1\}$, $n= \{0,1,\dots,N/2^{j+1}-1\}$, and $LL_0[n][m]$.

The decomposition is applied at different level repeatedly only low frequency channels (LL) to obtain next level decomposition. The term layer indicates both intermediate and output signals, while level is used for each decomposition stage. Four sub-bands in DWT are LL,LH,HL and HH obtained by applying DWT on keystroke dynamics data. The LL sub-bands corresponds to low frequency components of the keystroke time series and HL, LH and HH are high frequency component of the time series corresponding to vertical horizontal and diagonal sub-bands respectively. The LL sub-band we obtain is half the original data

GRAY-LEVEL CO-OCCURRENCE MATRIX (GLCM)

In statistical texture analysis, texture features are computed from the statistical distribution of observed combinations of intensities at specified positions relative to each other in the image. GLCM directions Analysis are 1. Horizontal (0°) 2. Vertical (90°) 3. Diagonal (a) Bottom left to top right (45°) (b) Top left to bottom right (135°). The distance and angular relationship in a sub-region of specific region can be represented with a specific size using GLCM³. The GLCM matrix can be formed from a gray scale image. How the intensity value occurs in an image can be calculated through GLCM. It represents how the intensity 'i' occurs, that is either horizontally or vertically, or diagonally to adjacent pixels intensity.

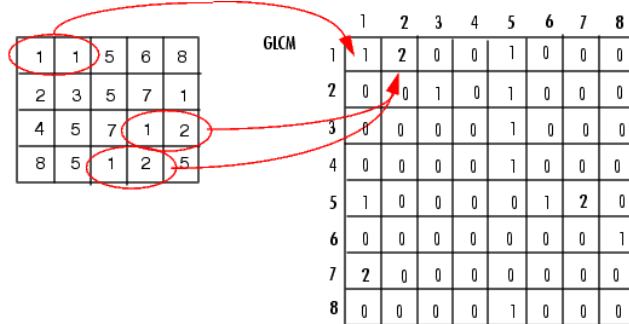


Figure:9 GLCM

CLASSIFICATION

In order to overcome the limitation of earlier neural networks, Professor Geoffrey Hinton introduces Deep Belief Networks⁶. DBN consists of two different types of neural networks – Belief Networks and Restricted Boltzmann Machines. In contrast to perceptron and backpropagation neural networks, DBN is unsupervised learning algorithm.

Restricted boltzmann machines

Boltzmann Machine is a stochastic recurrent neural network with stochastic binary units and undirected edges between units. Unfortunately, learning for Boltzmann machines is impractical and has a scalability issue⁷. As a result, Restricted Boltzmann Machine (RBM) has been introduced, which has one layer of hidden units and restricts connections between hidden units. This allows for more efficient learning algorithm.

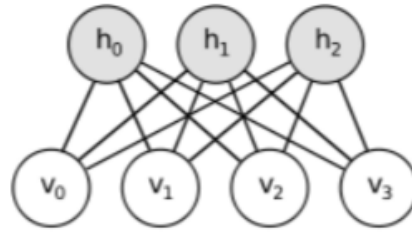


Figure: 10The structure of RBM

The above Fig. 10 shows the architecture of DBN⁶. Training of a DBN consists of two stages that allow learning feature hierarchies⁸. In the first stage, generative unsupervised learning is performed layer-wise on RBMs. First, a RBM is trained on the data. Second, its hidden units are used as input to another RBM, which is trained on them. In the second stage, discriminative fine-tuning using backpropagation is performed on the entire DBN to tweak the weights. Because of the pre-training, the weights have a good initialization, which allows back propagation to quickly optimize the weights.

Pre-training

A simple RBM with four input units and three hidden units has been used in this system. The unit in the visual layer is real value. The hidden units are typically binary stochastic variables, i.e, $h \in \{0, 1\}$. The Gaussian RBM is chosen for the first layer of RBM to model the real values of the keystroke features. The value of input and hidden variable, $\{v, h\}$, defines the state of the machine and the energy of the state, E , is defined as

$$E(v, h; \theta) = \sum_{i=1}^D \frac{(v_i - b_i)^2}{2\sigma_i^2} - \sum_{i=1}^D \sum_{j=1}^F w_{ij} \frac{v_i h_j}{\sigma_i} - \sum_{j=1}^F a_j h_j$$

Where $\theta = \{W, a, b, \sigma\}$ are parameters specifying the RBM. D is the number of input units, which is equal to the keystroke feature dimension. F is a user defined parameter specifying the number of hidden units, a is a weight vector for the hidden units, while b and σ are bias and variance parameters for the input layer. The value of F specifies the capacity of the model. It depends on the data complexity and amount of data available to train the parameters. The binary output of the first layer Gaussian RBM further serves as input for higher level RBMs to capture more complex non-linear structure embedded in the data. Higher level RBMs in the hierarchical generative are all defined as binary RBMs, i.e., both the visible and hidden layers contain only binary units. Their energy functions are defined as

$$E(v, h; \theta) = -v^T W h - b^T v - a^T h = - \sum_{i=1}^D \sum_{j=1}^F W_{ij} v_i h_j - \sum_{i=1}^D b_i v_i - \sum_{j=1}^F a_j h_j$$

The RBMs are stochastic and the joint distribution of visible and hidden units is,

$$P(v, h; \theta) = \frac{\exp(-E(v, h; \theta))}{z(\theta)}$$

Where $z(\theta)$ =is the normalization factor, known as partition function and can be defined as

$$z(\theta) = \sum_v \sum_h \exp(-E(v, h; \theta))$$

The likelihood of the training data is then is then specified as

$$P(v; \theta) = \frac{\sum_h \exp(-E(v, h; \theta))}{z(\theta)}$$

Fine tuning

The DBNN discriminative fine tuning solves a non-linear optimization problem. Pre-trained DBNs usually already have a good classification rate, as their feature detectors are learned from the training data. The cost function can be minimum classification error or reconstruction error depending on classification problem⁹. For large training data set, it is more efficient to compute the derivatives on a small, random mini-batch of training cases. In addition, the learning rate parameters, which can vary during the training process, need to be chosen carefully to balance training speed and avoid divergence¹⁰.

EXPERIMENTAL RESULTS

Dataset

Oral cancer is the cancer that starts in the mouth or oral cavity and is especially seen disadvantaged in elderly males. It is one among the 10 most common cancers worldwide, with 280,000 new cases of oral cancer found every year. It has been one of the serious cancers that affect the South Asian Countries. We have collected dataset from 100 cases from Raja Muttiah Dental College and Hospital. From the selected dataset 70% data is used for training, 15% data for testing and remaining 15% data is used for validation.

Performance Analysis

The experimental results is shown that the proposed method work in complex situation. True positive (TP) represents total number of correctly identified lane-mark edges by using the proposed approach. False positive (FP) represents the total number of in-correctly identified lane mark edges by using the proposed approach¹¹.

True Positive Rate (TPR) or Precision is defined as,

$$Precision = \frac{TP}{TP + FP}$$

Recall is defined as,

$$Recall = \frac{TP}{TP + FN}$$

Where, TP and FN are True Positive and False Negative. False Negative (FN) represents the total number of false detections. To compute, F-measure is defined as,

$$F - Measure = \frac{2 \times Recall \times Precision}{Recall + Precision}$$

The below table show the values of each variants of OSCC.

Table I. The overall detection for ANN gives an accuracy of 87.92% using dataset(ANN)

TYPE	Precision	Specificity	Sensitivity	Accuracy	Error Rate
ASCC	0.9200	0.8689	0.9388	0.9119	0.0881
PSCC	0.8861	0.5263	0.9091	0.8333	0.1667
SC	0.8333	0.7500	0.9091	0.8421	0.1579
BSCC	0.9695	0.9130	0.9407	0.9337	0.0663
VC	0.8774	0.7547	0.9394	0.8750	0.1250

Table II. The overall detection for DBM gives an accuracy of 93.37% using dataset (DBM)

TYPE	Precision	Specificity	Sensitivity	Accuracy	Error Rate
ASCC	0.7692	0.9423	0.7692	0.9076	0.0924
PSCC	0.9230	0.9801	0.8275	0.9461	0.0539
SC	0.7692	0.9449	0.8333	0.9461	0.0539
BSCC	0.7307	0.9345	0.8260	0.9153	0.8470
VC	0.9230	0.9803	0.8571	0.9538	0.0462

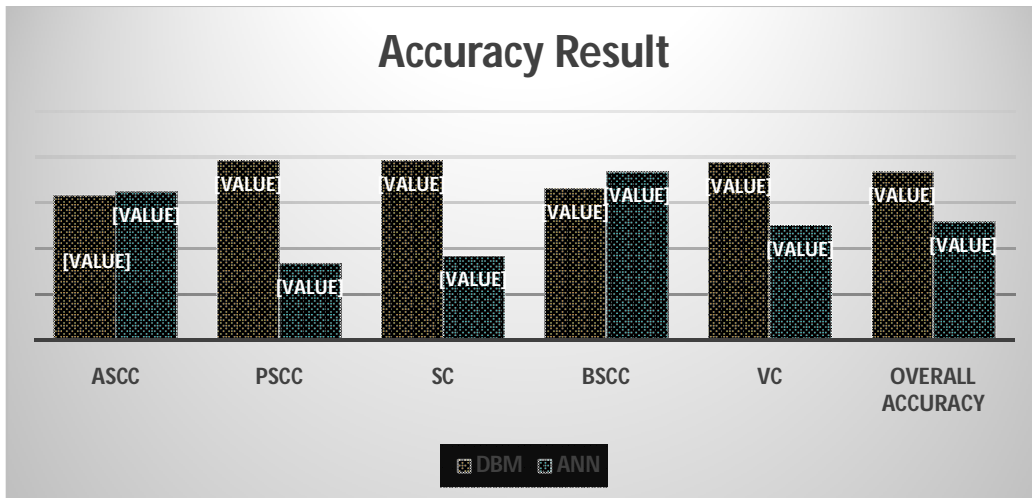


Figure11: Comparison between existing and proposed result

The above figure shows the maximum accuracy achieved in DBM classifier.

CONCLUSION

In this paper, an attempt is made to classify the microscopic images of oral squamous cell carcinoma from histopathological slides into variants types of OSCC. The texture features of the images are considered for performing the classification. The approaches used for DWT is a powerful tool for signal-processing and image processing. Due to simplicity and minimum computational complexity, DWT is more suitable for the extraction of features from images. GLCM is one of the well-known feature extractor to extract features. The proposed approach is classified with DBM classifier. It is a deep learning classifier. Computational time will also be considered to compare this technique efficiently. As the diagnosis cancer is a complicated and sensitive task, accuracy and reliability are always assigned much importance. The result of the proposed system is compared with the existing work of ANN classification. The existing work gave 87.92% of accuracy, but the proposed work gives 93.37% of accuracy, and it is proved that the proposed work is better than the existing work.

REFERENCES

1. MuzakkirAhmed .C.R, Narayanan .M,Kalaivanan .S, Sathyanan .K,Reshmy .A.K, “To Detect And Classify Algorithm and ExpectationMaximization Algorithm”, International Journal of Pure and Applied Mathematics, 2017;116(21):149-154.
2. Aurchana .P,Dhanalakshmi .P,Indhumathi .J, “Histopathological Variants of Oral Squamous Cell Carcinoma using Artificial Neural Network”, International Journal of Scientific Research in Computer Science Applications And Management Studies, 2018;7(5):2319-1953.
3. Anuradha .K, ‘Efficient oral cancer classification using GLCM feature extraction and fuzzy cognitive map from dental radiographs’, International Journal of Pure and Applied Mathematics, 2018;118(20):651-655.
4. Anuradha.K, Sankaranarayanan.K, “Identification of suspicious regions to detect oral cancers at an earlier stage – A literature survey”. International Journal of Advances in Engineering and Technology, 2012;3(1):84-91.
5. NarayanNaik, Anusha Amin, Dechamma .K.C, Deepthi.B.A, NidhiHegde, may,“Oral Cancer Detection Using Android Application. International Journal of Advanced Research in Computer Science and Software Engineering”, 2017;7(5):108 – 111.
6. Anuradha.K, Sankaranarayanan.K, ‘Comparison of Feature Extraction Techniques to classify oral cancers using Image Processing’. International Journal of Application or Innovation in Engineering and Management,2013;2(6):456 – 462.

7. Mahmud .M, Kaiser .M.S, A. Hussain, S. Vassanelli, “Applications of Deep Learning and Reinforcement Learning to Biological Data”, IEEE Transactions on Neural Networks and Learning Systems, 2018;29(6):2063-2079.
8. Anuradha.K, Uma.K.P, ‘Histological grading of Oral Tumors using Fuzzy Cognitive Map, Biomedical and Pharmacology Journal’,2017;10(4):1695 – 1700.
9. Abdulkader M. Albasri, Abdulrahman H. Ali and Ayesha A. Nathiha, ‘Segmentation of immunohistochemical staining of β -catenin expression of oral cancer using EM algorithm’, Journal of Taibah University Medical Sciences, 2015;2(2):169-174.
10. Khalid Raza and NripendraKumar Singh, “A Tour of Unsupervised Deep Learning for Medical Image Analysis”, IEEE Trans. Med. Imaging, 2018;35:119-130.
11. Kulhalli .K.V,Patil .V.TandUdupi .V.R, “Image Processing Application for Computer aidedDiagnosis of Cancer”, Image Processing Application for Computer aided Diagnosis of Cancer, 2016:1:297-308.